Probing Anomalous HVV Couplings at the FCC-eh

FCC Week 2017, 29 May - 2 June
Berlin, Germany

M. Altinli [1], I. Turk Cakir [2], O. Bolukbasi [1], A. Senol [3], S. Kartal [1], O. Cakir [4]
[1] Istanbul University, [2] Giresun University, [3] Abant Izzet Baysal University, [4] Ankara University

Abstract

In this study, we have investigated Higgs-gauge boson couplings via $e^-p \to e^-q\,H$ process at the Future Circular electron-hadron Collider (FCC-eh). The bounds on the anomalous HVV couplings in this process are obtained by using MadGraph5 framework at the FCC-eh. The results are compared with the results obtained at the Large Hadron electron Collider (LHeC).

Introduction

The recent discovery of a new boson with a mass of 125 GeV at the CERN LHC [1, 2] matches many of the properties of the Higgs boson from the Higgs mechanism within the Standard Model (SM). Searching for the properties of this new boson can extend our knowledge of the electroweak symmetry breaking (EWSB) sector. This search has also very important consequences on theories beyond the SM. From the theoretical side, there could be different EWSB scenarios in which the Higgs boson can be elementary and weakly interacting [3] or composite and related to a new strongly interacting sector [4]. Effects of EWSB scenarios on the phenomenology of the Higgs boson can be parameterized in terms of an effective Lagrangian at the electroweak scale. In this framework, the corrections from higher dimensional operators to the Higgs boson (H) couplings to the gauge bosons (V) can be expressed through an effective Lagrangian. The effective operators give rise to anomalous HVV couplings [5].

$$\begin{aligned}\mathcal{L}_{eff} = &-\frac{1}{4}g_{h\gamma\gamma}F_{\mu\nu}F^{\mu\nu}h - \frac{1}{4}\tilde{g}_{h\gamma\gamma}F_{\mu\nu}\tilde{F}^{\mu\nu}h - \frac{1}{4}g^{(1)}_{hzz}Z_{\mu\nu}Z^{\mu\nu}h \\ &- g^{(2)}_{hzz}Z_{\nu}\partial_{\mu}Z^{\mu\nu}h + \frac{1}{2}g^{(3)}_{hzz}Z_{\mu}Z^{\mu}h - \frac{1}{4}\tilde{g}_{hzz}Z_{\mu\nu}\tilde{Z}^{\mu\nu}h \\ &- \frac{1}{2}g^{(1)}_{haz}Z_{\mu\nu}F^{\mu\nu}h - \frac{1}{2}\tilde{g}_{haz}Z_{\mu\nu}\tilde{F}^{\mu\nu}h - g^{(2)}_{haz}Z_{\nu}\partial_{\mu}F^{\mu\nu}h\end{aligned} \tag{1}$$

Where $V_{\mu\nu}$ is the field strength tensor and V_μ is the vector field. Effective couplings are denoted by g_{hvv} .

Hγγ, HZZ and HγZ Couplings

The couplings appearing in the effective Lagrangian are given as in Table 1. The related diagrams for the $e^-p \to e^-q\,H$ which contain Hγγ, HZZ and HγZ interaction vertices are shown in Figure 1.

Table 1. Coupling constants of the interactions of a Higgs boson with a vector boson pair.

$g_{h\gamma\gamma}$	$a_H - \frac{8g\bar{c}_\gamma s_W^2}{m_W}$
$\tilde{g}_{h\gamma\gamma}$	$-\frac{8g\tilde{c}_\gamma s_W^2}{m_W}$
$g^{(1)}_{hzz}$	$\frac{2g}{c_W^2 m_W}\left[\bar{c}_{HB}s_W^2 - 4\bar{c}_\gamma s_W^4 + c_W^2\bar{c}_{HW}\right]$
$\tilde{g}_{hzz}$	$\frac{2g}{c_W^2 m_W}\left[\tilde{c}_{HB}s_W^2 - 4\tilde{c}_\gamma s_W^4 + c_W^2\tilde{c}_{HW}\right]$
$g^{(2)}_{hzz}$	$\frac{2g}{c_W^2 m_W}\left[\left(\bar{c}_{HW} + \bar{c}_W\right)c_W^2 + \left(\bar{c}_B + \bar{c}_{HB}\right)s_W^2\right]$
$g^{(3)}_{hzz}$	$\frac{g m_W}{c_W^2}\left[1 - \frac{1}{2}\bar{c}_H - 2\bar{c}_T + 8\bar{c}_\gamma\frac{s_W^4}{c_W^2}\right]$
$g^{(1)}_{haz}$	$\frac{g s_W}{c_W m_W}\left[\bar{c}_{HW} - \bar{c}_{HB} + 8\bar{c}_\gamma s_W^2\right]$
$\tilde{g}_{haz}$	$\frac{g s_W}{c_W m_W}\left[\tilde{c}_{HW} - \tilde{c}_{HB} + 8\tilde{c}_\gamma s_W^2\right]$
$g^{(2)}_{haz}$	$\frac{g s_W}{c_W m_W}\left[\bar{c}_{HW} - \bar{c}_{HB} - \bar{c}_B + \bar{c}_W\right]$

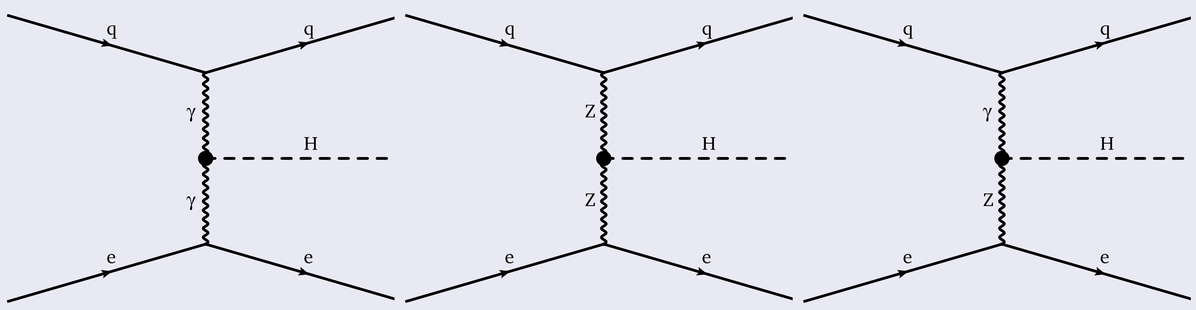

Figure 1. Feynman diagrams of $e^-p \to e^-q\,H$ process, that include Hγγ, HZZ and HγZ vertices.

In this study, we used $e^-p \to e^-q\,H$ process to investigate all the parameters that contribute to the Hγγ, HZZ and HγZ interaction vertices. We investigated each parameter in range [-0.1, 0.1] while other parameters were set to zero. We used MadGraph5_aMC@NLO (v2.3.3) [6] to generate the signal and background events with the effective Lagrangian implementation through FeynRules [7]. We also used Pythia (v6.428) for hadronisation and Delphes (v3.3.0) for detector simulation. All the calculations have been performed with and without the polarisation of the electron.The initial parameters for electron energy 60 GeV and proton energy 7 TeV were used at the LHeC while electron energy 60 GeV and proton energy 50 TeV were used at the FCC-eh.

Analysis

Invariant mass distributions of two b-jets are shown in Figure 2 and Figure 3. Figure 3 is for the processes with left-handed (80%) polarized electron while Figure 2 is for the processes without polarisation. For the signal processes, we take $\bar{c}_{HW}$ = -0.03 while all other couplings are zero. We have used 1 ab^{-1} integrated luminosity and we applied cuts $p_T^j > 60$ GeV, $-4.5 < \eta^j < 0$, $0.5 < \Delta R_{bb} < 2$ and $|\eta^e| < 2$ to the electron and jets. We take into account background $B \supset e^-q\,H, e^-q\,Z, e^-q\,W^\pm, e^-W^\pm t(\bar{t}), e^-t\,\bar{t}$.

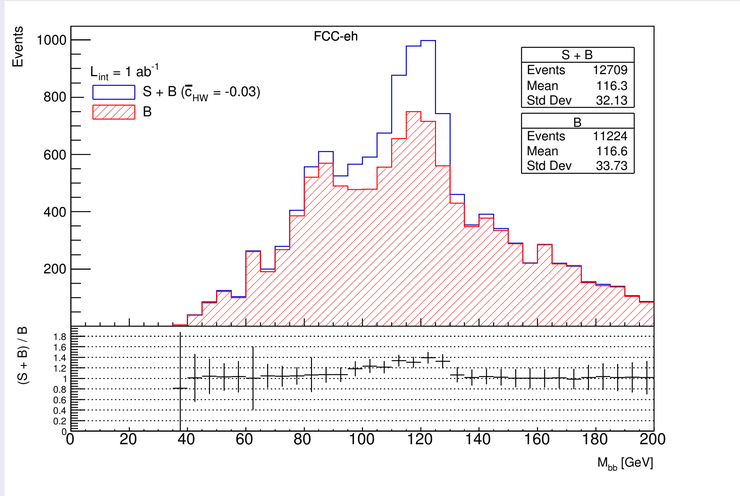

Figure 2. Invariant mass of two b-jets for $\bar{c}_{HW}$ = -0.03 at FCC-eh.

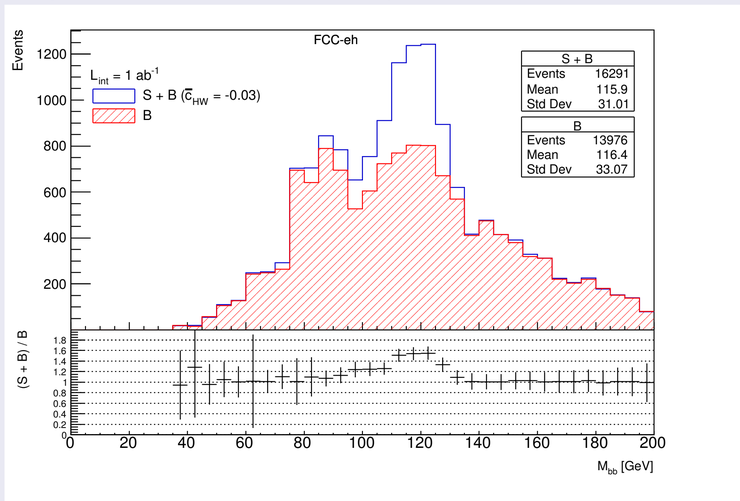

Figure 3. The same as Figure 2 but for 80% left-handed electron polarisation.

Results

We used the number of the signal (S) and background (B) events to calculate the statistical significance defined as

$$SS = \sqrt{2[(S+B)\ln\left(1+\frac{S}{B}\right) - S]} \tag{2}$$

In Figure 4 and 5, the statistical significance for anomalous coupling values, -0.05 and 0.05, are shown at LHeC and FCC-eh for 1 ab^{-1} luminosity.

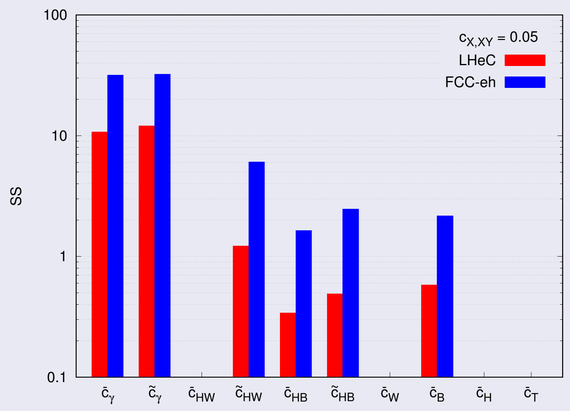

Figure 4. SS plot for anomalous couplings while $c_{X,XY}$ = 0.05 at LHeC and FCC-eh.

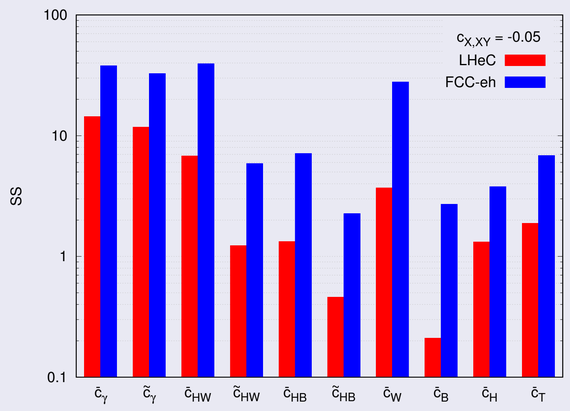

Figure 5. SS plot for anomalous couplings while $c_{X,XY}$ = -0.05 at LHeC and FCC-eh.

Conclusion

We have investigated couplings relevant to anomalous HVV vertices at the LHeC and the FCC-eh. The results show that LHeC and FCC-eh provide a better sensitivity to the $\bar{c}_\gamma$, $\tilde{c}_\gamma$ couplings. We find that the FCC-eh collider is more sensitive to the anomalous couplings than LHeC due to higher center of mass energy, however the polarisation possibility of the electron beam has an advantage for charged/neutral weak current process for both cases. Our results can be compared with the results from experimental bounds [8] and phenomenological results [9]. The ep colliders will complement these searches.

References

[1] G. Aad et al. (ATLAS Collaboration), Phys. Lett. B 716,1 (2012).
[2] S. Chatrchyan et al. (CMS Collaboration), Phys. Lett. B 716, 30 (2012).
[3] G. Altarelli, arXiv: 1206.1476.
[4] S. Dimopoulos, and L. Susskind, Nucl. Phys. B 155, 237 (1979); S. Weinberg, Phys. Rev. D19, 1277 (1979).
[5] T. Corbett et al., Phys. Rev. D 86, 075013 (2012); T. Corbett et al., Phys. Rev. D 87, 015022 (2013).
[6] J. Alwall et al., JHEP 1407 (2014) 079.
[7] A. Alloul, B. Fuks and V. Sanz, JHEP 04 (2014) 110.
[8] ATLAS Collaboration, Physics Letters B 753 (2016) 69-85.
[9] I. T. Cakir, O. Cakir, A. Senol, A. T. Tasci, Mod. Phys. Lett. A, Vol. 28, No. 31, 1350142 (2013)